



NCAR



Motivation: Accurate specification of the magnetosphere-ionosphere (MI) coupling is crucial in modeling the thermosphere-ionosphere (TI) response to geomagnetic activity, in general circulation models (GCM) the MI coupling is typically realized by specifying the ion convection/potential patterns based on empirical models. Due to the availability of AMPERE data there is an increased interest in driving GCMs by field-aligned current (FAC) to represent MI coupling. As with specifying the high latitude potential pattern the main issue is the consistency between the particle precipitation patterns and the potential/FAC patterns since they are in general not derived in a self-consistent way.
Focused study goal: In the following, we want to determine the sensitivity of the high- and low latitude ionosphere to changes in aurora conductivities if a high latitude electric potential or FAC pattern is specified.
We present the impact on the GCM results for the different MI forcing cases.

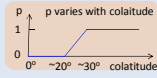
Method

We create a controlled simulation experiment by defining a FAC J_{Mr}^R in such a way that it creates the same electric potential solution Φ as forcing by a high latitude potential Φ^R does. We will simulate only one time-step to isolate the thermosphere-ionosphere (TI) effect of modified conductances in the potential (POT) and FAC (FAC) forcing case, and thereby exclude possible changes due to feedback from the TI.

Steady state ionospheric electrodynamics

Potential (POT) case

$$p \frac{\partial}{\partial \phi_m} \left[\frac{\Sigma_{\phi}^R}{\cos \lambda_m} \frac{\partial \Phi}{\partial \phi_m} + \Sigma_{\phi}^T \frac{\partial \Phi}{\partial \lambda_m} \right] + p \frac{\partial}{\partial \lambda_m} \left[\Sigma_{\phi}^T \frac{\partial \Phi}{\partial \phi_m} + \Sigma_{\lambda}^R \cos \lambda_m \frac{\partial \Phi}{\partial \lambda_m} \right] = pR \left[\frac{\partial K_{\phi}^{DT}}{\partial \phi_m} + \frac{\partial K_{\lambda}^{DT}}{\partial \lambda_m} \cos \lambda_m \right] - (1-p) \sigma^R R \cos \lambda_m \Phi$$



Field-aligned current (FAC) case

$$\frac{\partial}{\partial \phi_m} \left[\frac{\Sigma_{\phi}^R}{\cos \lambda_m} \frac{\partial \Phi}{\partial \phi_m} + \Sigma_{\phi}^T \frac{\partial \Phi}{\partial \lambda_m} \right] + \frac{\partial}{\partial \lambda_m} \left[\Sigma_{\phi}^T \frac{\partial \Phi}{\partial \phi_m} + \Sigma_{\lambda}^R \cos \lambda_m \frac{\partial \Phi}{\partial \lambda_m} \right] = R \left[\frac{\partial K_{\phi}^{DT}}{\partial \phi_m} + \frac{\partial K_{\lambda}^{DT}}{\partial \lambda_m} \cos \lambda_m \right] + J_{Mr}^R R^2 \cos \lambda_m$$

Note: Specifying a potential or FAC describes the MI coupling as a pure voltage (where p=0) or current generator, respectively. This is an idealized way to describe the magnetosphere-ionosphere coupling since ionospheric conductivities and the dynamo impose restrictions on the relation between electric fields and FAC, and the magnetospheric plasma pressure and plasma acceleration also constrain the FAC to the ionosphere. Specifying a potential or FAC at high latitude doesn't in general satisfy the ionospheric and magnetospheric constraints simultaneously.

Controlled experiment

Potential [kV] day-70 UT-0 min-1

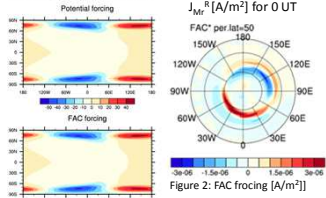


Figure 1: electric potential [kV] resulting in identical electric potential solution. Figure 2 illustrates the J_{Mr}^R forcing which gives the identical electric potential Φ in Fig. 1 which represents the reference case (REF).

To get the same potential solution Φ with a potential forcing and a J_{Mr}^R forcing we first prescribe a potential pattern Φ^R at high latitude using Eq. (1) and find the potential solution Φ which is then used to calculate J_{Mr}^R with Eq. (2). J_{Mr}^R is employed in the FAC case (Eq. 2) as forcing.

The electric potential solution is illustrated in Fig.1 forced by a specified electric potential (top) and by FAC (bottom)

Summary:

We conducted a controlled experiment by forcing with a high latitude electric potential Φ^R (POT case) and field-aligned current J_{Mr}^R (FAC case) producing the same electric potential solution Φ . We modified the auroral conductivities for our controlled experiment to test the sensitivity of different quantities when forced by a high latitude electric potential and field-aligned current.

- In the POT case (electric potential Φ^R prescribed) the hemispheric integrated Joule heating is more sensitive to conductance changes than in FAC case (J_{Mr}^R prescribed) (see Fig. 5,7,9).
 - In the FAC case (J_{Mr}^R prescribed) the high latitude electric field changes are in general anti-correlated to the conductance modifications (Fig. 3), leading to smaller Joule heating changes compared to the POT case (electric potential Φ^R prescribed) (Fig. 5).
 - The equatorial vertical ExB drift exhibits larger changes in the FAC case compared to the POT case (Fig. 11), related to the fact that the electric field needs to be adjusted at high latitude in the FAC case. However, the penetration electric field tends to be larger in the POT case than in the FAC case (Fig. 10).
 - The largest equatorial vertical drift changes in the FAC case are during the night time (Fig. 11) and do not necessarily correlate with the magnitude of the conductance changes.
- As a next step we want to examine the effects of modified conductivities over a longer time period. The changes in the Joule heating may influence the global circulation, mid-latitude plasma distribution as well as polar neutral densities. The modifications in the equatorial vertical ExB drift may influence the low latitude plasma distribution and ion-neutral coupling, however, the largest drift changes are at night time.

Effect of aurora conductivity modifications on high latitude electric field

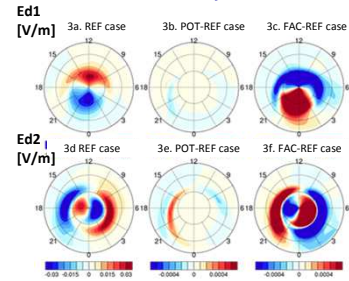


Figure 3: Eastward electric field Ed1 [V/m] 3a-c; equator/downward electric field Ed2 [V/m] 3d-f; total electric field from REF case 3a & 3d; difference electric fields 1b-c & 2b-c.

- An increase in auroral conductance leads to
- A decrease in electric fields for the FAC case (Figure 3 c & f) since the field aligned current is prescribed.
- No change in the polar electric field for the POT case (Figure 3 b & e) since the electric potential is prescribed. However, equatorward of the ion convection reversal boundary there are changes.

Effect of aurora conductivity modifications on Joule heating

Case B: Increase in auroral radius by 2.5°

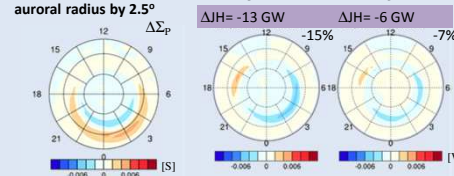


Figure 7: Case B: Pedersen conductance changes Σ_p [S].

Effect on penetration electric fields (PEF)

Vertical ExB drift [m/s] for 0 UT at $\lambda_E = 0^\circ$ & ~400km

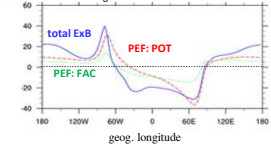


Figure 10: Total ExB drift [m/s] & PEF for POT & FAC case

- The PEF are determined by setting the wind dynamo terms K to zero in Eq. (1) and Eq. (2).
- The penetration electric field effect for the POT and FAC case differ (Fig. 10 red and green line, respectively).
- In the POT case the factor p (see Eq.(1)) varies with colatitude.

Case A: Increase in auroral conductance

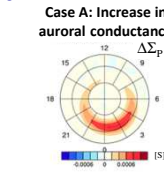


Figure 4: Case A: Pedersen conductance changes Σ_p [S]. The auroral Pedersen conductance is increased by max. 7%.

Rate of energy transfer

$$J_{\perp} \cdot E = J_{\perp} \cdot E' + u \cdot (J_{\perp} \times B)$$

Joule heating Mechanical work (MW)

with E' in the neutral wind frame $E' = E + u \times B$ and u the neutral wind
Rate of energy transfer changes for POT case by ~7%; for FAC case by 1.2%
Joule heating is changing for POT case by ~7%; for FAC case by 1.9%
Mechanical work is changing for POT case by 6%; for FAC case by -26%
Mechanical work on winds is very small with ~2% of total energy.

Effect on Joule heating & mechanical work

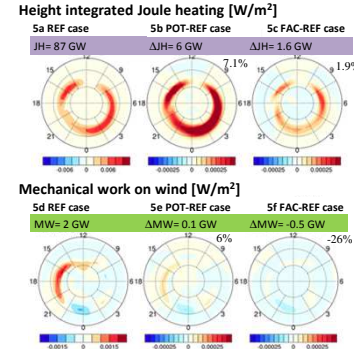


Figure 5: Joule heating [W/m^2] a-c; mechanical work [W/m^2] d-f.

Case C: Move aurora to dusk by 2.5°

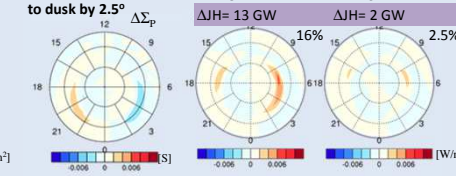


Figure 8: Case C: Pedersen conductance changes Σ_p [S].

Increase in auroral radius by 2.5°

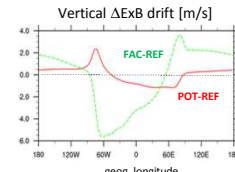


Figure 11: ExB drift changes [m/s] for conductance modifications Case B (left) and Case C (right).

Move aurora to dusk by 2.5°

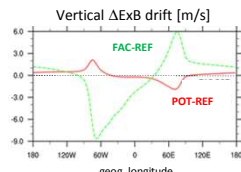


Figure 9: Case C Joule heating changes [W/m^2].

In general the equatorial ExB changes are smaller in POT than FAC case (Fig. 11) but the absolute penetration electric field effect is larger in the POT than FAC case (Fig. 10). The largest changes are during night time (Fig. 11).